**NASA
Technical
Paper
2117**

January 1983
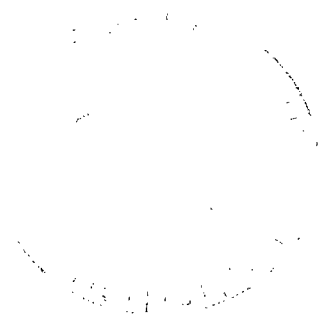
Identification and Management of Filament-Wound Case Stiffness Parameters

V. Verderaime
and M. Rheinfurth
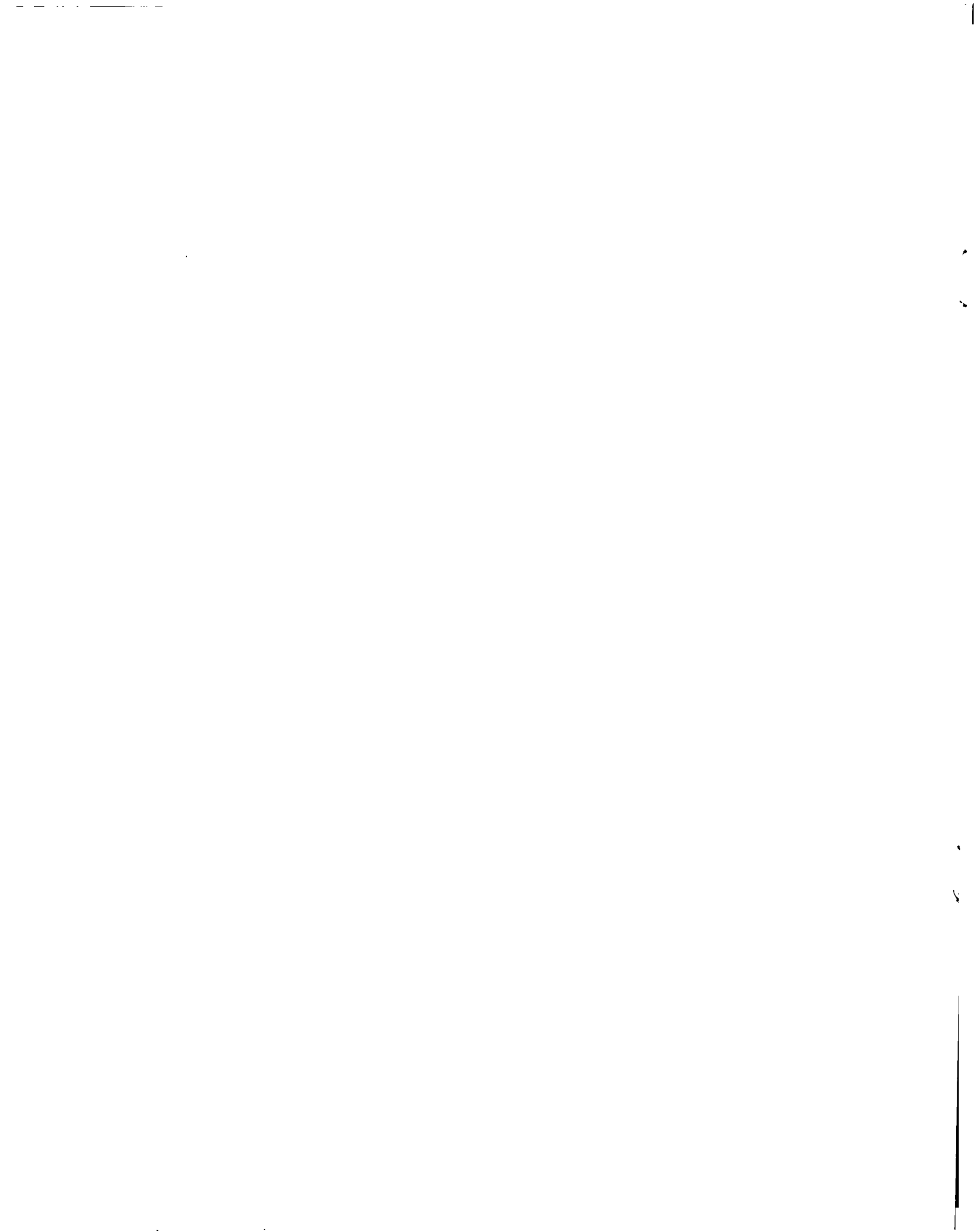
NASA

NASA
Technical
Paper
2117

1983

Identification and Management of Filament-Wound Case Stiffness Parameters

V. Verderaime
and M. Rheinfurth
George C. Marshall Space Flight Center
Marshall Space Flight Center, Alabama

TABLE OF CONTENTS

LIST OF ILLUSTRATIONS

LIST OF SYMBOLS

A_{ij} engineering constants, predicted

a axial acceleration

c_n test result constant

$E_{ij}, \hat{E}_{ij}$ in-plane tension modulus, predicted and observed, respectively

G_{12} in-plane shear modulus

g_n constraint equation

L motor case cylinder length between end closures

ΔL motor case axial growth

P hydrostatic pressure

P_c combustion chamber pressure

$\dot{P}_c$ chamber pressure rise rate

S_{ij} engineering constants observed

T solid rocket motor thrust corresponding to P_c

t motor case mean thickness

ϵ_1, ϵ_2 axial and hoop strains, respectively

λ_n Lagrange multiplier

ν_{12} Poisson's ratio, hoop contraction under axial load

σ_1, σ_2 axial and hoop stress, respectively

Subscript

$1, 2$ axial and hoop directions, respectively

TECHNICAL PAPER

IDENTIFICATION AND MANAGEMENT OF FILAMENT-WOUND
CASE STIFFNESS PARAMETERS

INTRODUCTION

The promise of high specific strength and high specific stiffness of filament-wound pressure vessels is responsible for reexamination of structural material selection for space vehicles. A recent study concluded that an 18 percent increase in Space Shuttle payload may be realized by substituting steel structural segments of the solid rocket motor case with graphite-epoxy laminate. This change utilizes about 15 metric tons of graphite laminate per motor case making it the largest filament winding application to be flown on a single mission. Of equal distinction is that the Shuttle structural interface optimization with the steel motor case established many constraints unfavorable to the laminate case and a respectable payload increase was still projected.

The most consequential employment of graphite epoxy was its accommodation to existing manufacturing and processing methods and to operational environments. New demands on technology were the segmented case joint strength and seal integrity and the unique axial stiffness constraint. Every precaution to avoid technical surprises and, therefore, reduce schedule risks was thoroughly exercised by all associated spacecraft disciplines. However, this report documents only the identification and verification approaches to structural stiffness problems that contrasted from the existing solid motor steel case dynamics. Included is an innovative experimental analysis application to specially orthotropic membranes for verifying the constitutive parameters, nondestructively.

FILAMENT-WOUND CASE CONFIGURATION

The fundamental Shuttle operational requirement was the interchangeability of the solid motor filament-wound case with the existing steel motor case. This implied that physical interfaces with Shuttle elements and booster major components had to remain intact and interfaces with facilities and handling equipment had to be minimized. It further implied that loads and dynamic effects transmitted through interface structures could not exceed those induced by the existing operational steel motor case.

Three motor case steel components were unchanged. First the steel aft dome was not changed to a graphite laminate because the thrust vector control system requirement on local structural stiffness returned no weight advantage. Second, the steel case segment with the external tank attach ring was also retained because the thicker laminate shell would have increased the attach ring inside diameter and thus modified the aft interface dynamics with the external tank which has already been characterized through extensive, full scale dynamic testing. Third, the small weight savings, the adverse shift in mass center, and the extensive development estimated for the forward dome and skirt generated no incentive to convert the existing steel structure to a laminate.

The solid motor case net modification consisted of substituting 31 m total length of steel cylindrical shell to graphite filament-wound composite structure, as shown in Figure 1. The composite cylinder is fabricated in four segments to simplify handling, shipping, and propellant casting and to comply with existing field stacking and splicing facilities.
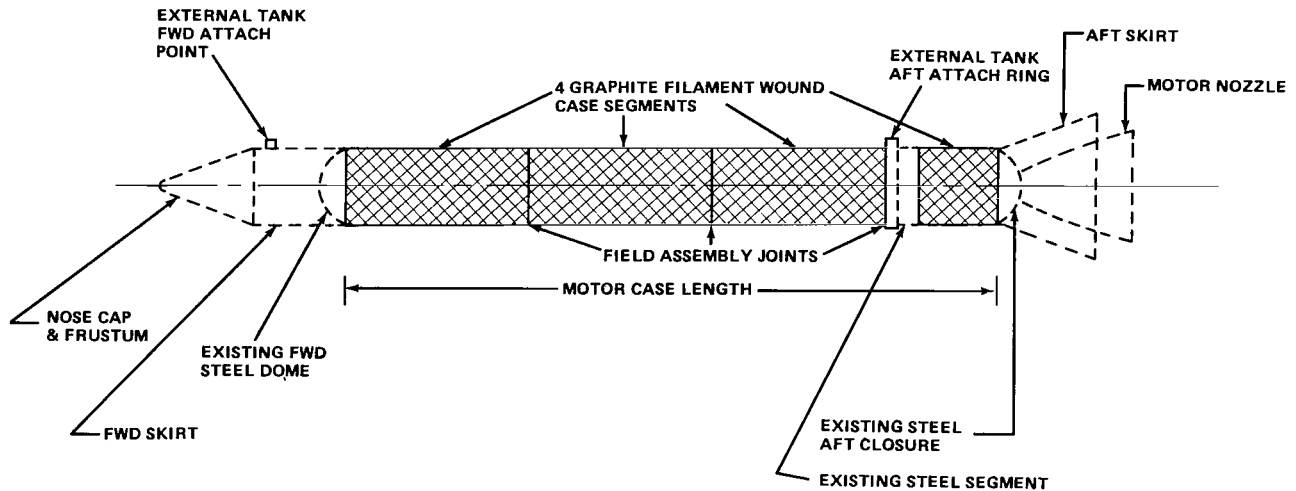
Figure 1. Solid rocket booster.

DESIGN STIFFNESS CRITERIA

The solid rocket motor case conversion to a composite structure caused very minor changes in Shuttle redistribution from the motor case to the payload, trivial envelop increase, and no measurable change in such forcing functions as thrust rise rates, misalignment, oscillations, gusts, and controls. Therefore, any Shuttle systems load changes or exceedance over the steel motor case configuration [1] had to be traced to the composite motor case changes in axial and flexural stiffness.

An early filament-wound case study predicted a payload increase of nearly 25 percent. The same interface loads developed for the steel motor case were assumed to apply and very liberal structural stiffnesses were specified. The case bending section modulus was reduced to two-thirds of that of the steel case. This reduction was limited by the vehicle control system requirement. The case axial elongation during thrust build-up was allowed to increase up to five times that of the steel case. However, it was concluded from subsequent systems load response analyses that the crew module and the external tank dome design limits were exceeded for all axial growth allowances greater than the existing steel case axial growth. This constraint was met with a thicker and heavier case laminate system with a corresponding payload increase of only 18 percent.

To understand this payload performance reduction, significant contrasts between the laminate and the steel case must be examined at liftoff condition. This condition occurs when the total thrust is equal to the total Shuttle weight within 0.25 sec after the solid rocket motor ignition. During this period of solid motor thrust buildup, the chamber pressure rises to half its maximum which causes the motor case to expand radially and axially at a very high rate. Since the solid rocket is constrained by the launch pad at the aft end (Fig. 2), the axial growth is directed forward. The external tank, which is attached at a point forward of the solid motor case, and the Orbiter, which in turn is attached to the external tank, experience a substantial forward acceleration which is related to the net axial growth of the motor case at time of liftoff and the chamber pressure rise rate,

$$a \sim \Delta L \, \dot{P}_c \tag{1}$$

2
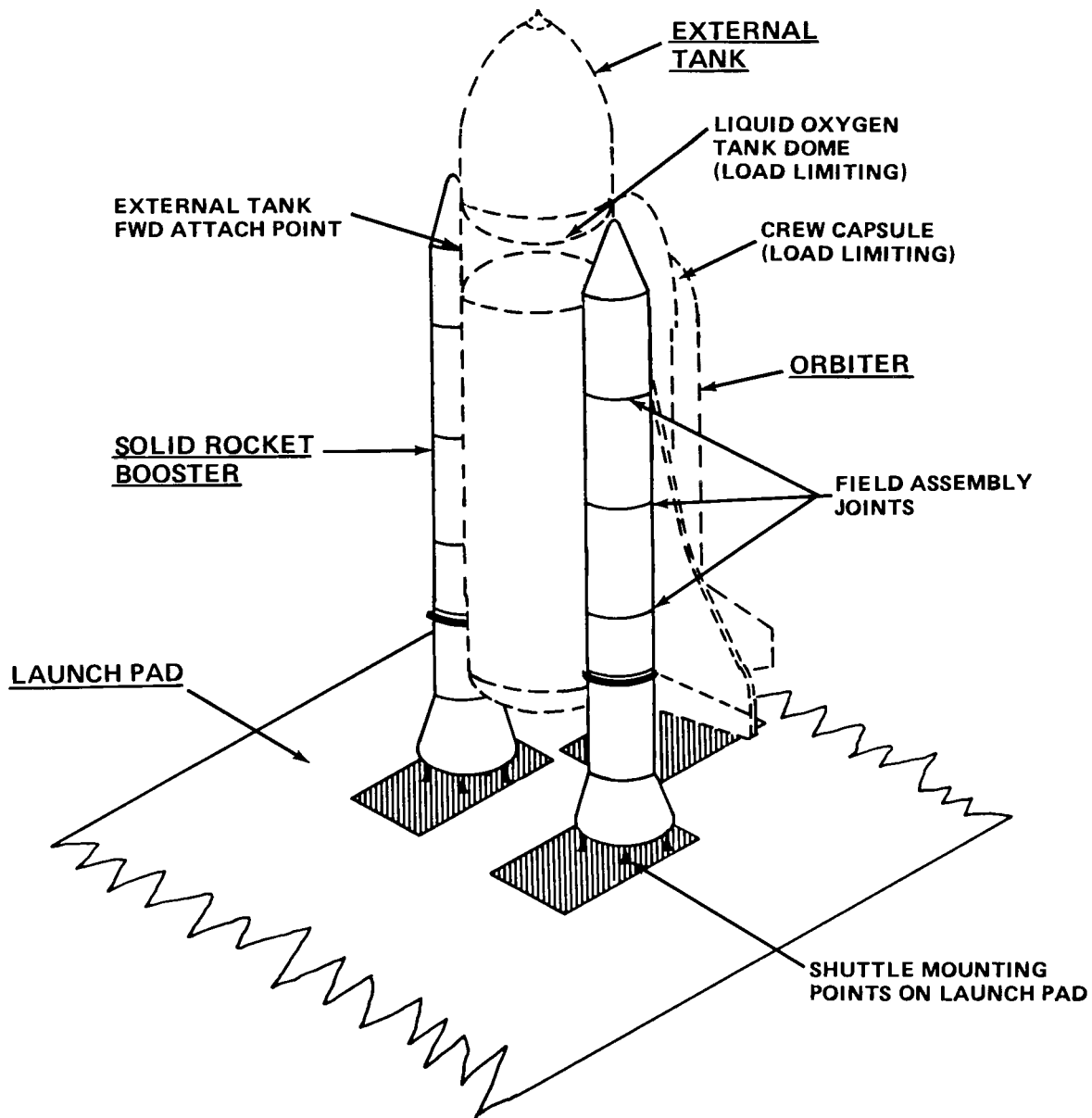
Figure 2. Shuttle configuration at lift-off.

This very brief ramp excitation is responsible for 40 percent of the external tank dome design limit load which was established by the existing steel motor case. Since the excitation of equation (1) could not be exceeded and the pressure rise rate was common to the filament-wound and steel motor cases, the axial growth also could not be exceeded.

To follow the nature of this axial constraint on the filament-wound case design, the motor case membrane elongation in the plane stress condition was expressed by

$$\Delta L = L\,\epsilon_1 = L\left[\frac{\sigma_1}{E_1} - \sigma_2 \frac{\nu_{21}}{E_2}\right]$$

or in specific motor case terms of geometry, loads and material properties as follows:

$$\Delta L = \frac{L}{\pi D E_1 t}\left[\frac{\pi}{4} D^2 P_c (1 - 2\nu_{12}) - T\right] \qquad . \tag{2}$$

As expected, the only parameters of equation (2) that were notably different between the two cases were those associated with the material properties. Though the graphite fiber modulus was comparable to steel, it was severely diminished when it was oriented and embedded into a graphite-epoxy laminate system that was optimized for maximum strength and stiffness with minimum weight. On the other hand, the laminate Poisson's ratio could be made to vary by an order of magnitude. To satisfy the minimum stiffness requirement imposed by the vehicle control system, the two-thirds bending section modulus of the filament-wound case meant reducing the product of axial modulus and thickness (E · t) by no less than two-thirds that of the steel case. That condition and the case structural integrity requirement were satisfied by using a Poisson's ratio of only one-tenth. A maximum payload increase was realized and no increase in twang liftoff loads was noted due to the sudden change from a cantilevered-mounted motor to free-free ends. However, the axial growth from equation (2) was five times that of the steel case and the axial excitation given by equation (1) increased accordingly.

Through further system loads response analyses and trade studies, the maximum axial elongation permitted at liftoff was confirmed to be equal to that of the steel motor case. The only parameter left to satisfy the axial growth constraint was the Poisson's ratio. Increasing it and satisfying the laminate case bending stiffness and strength severely penalized the payload potential.

STIFFNESS CONTROL PARAMETERS

Design standards, manufacturing processes, and operational exposures of the filament-wound case were reviewed to identify all parameters and potential degradation that affect axial growth. Parameter influence predictions and allowables were implemented into the motor case design, and verification methods were planned.

The four laminate segments are field-spliced by the existing steel clevis/tang joint concept and locked with interchangeable double shear pins. This type of field joint consists of a pair of steel rings adapted to the laminate shells by a similar tang/clevis arrangement (Fig. 3). The laminate segment ends are shaped into tangs and mated to the steel rings with double shear pins at the manufacturing plant. It has been estimated for the current steel motor case, that the pin-to-hole and hole "true position" tolerances and the plastic-elastic hole elongation accounts for 20 percent of the total case elongation at liftoff. Therefore, a comprehensive evaluation of all pin joints is necessary to minimize their effects on axial growth.

The hole "true position" tolerance is the pin hole centerline dispersion from a plane normal to the segment and ring axis. As this tolerance is increased, the pin-to-hole tolerance must also increase to facilitate the pin installation through the laminate tang and steel clevis holes. Increasing the "true position" tolerance

COMPOSITE SEGMENTS

CLEVIS END

TANG END

PIN-TO-HOLE
TOLERANCE

LOCAL STRAINS AND
HOLE ELONGATION

TRUE POSITION
TOLERANCE

STEEL CLEVIS

JOINT SEALS

STEEL FIELD
JOINT
(TANG AND CLEVIS)

TYPICAL COMPOSITE
SEGMENT JOINT
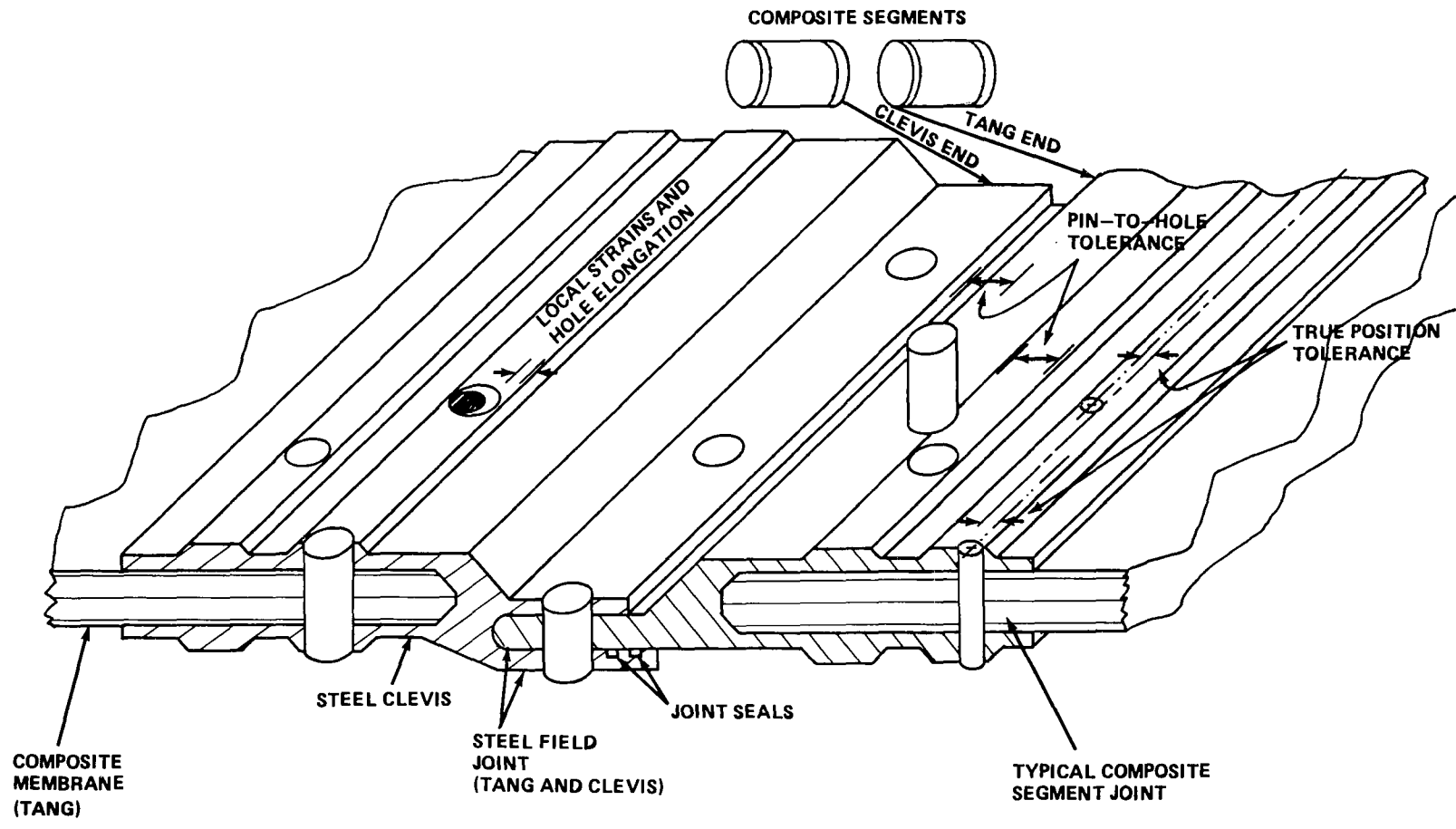
COMPOSITE
MEMBRANE
(TANG)

Figure 3. Filament-wound case joints.

also increases the laminate hole axial strain because of the statistically varying contact load distribution. Single pass drilling of the pin holes through the laminate and steel rings together may lead to an optimum solution.

After the laminate segment is connected to the steel joint ring, the segment is hydroproofed to verify the structural integrity and axial growth compliance. This is the last axial stiffness inspection. It is then prepared for integration with the propellant which consists of bonding a rubber insulating liner onto the inner surface of the segment before casting the grain. The segment and liner are then subjected to a vulcanizing temperature of over 120°C. The joint pin diameter expansion is greater than the graphite-epoxy laminate hole which effects pin-to-hole tolerance degradation that inadvertently exceeded the segment elongation specification after it was inspected. This expansion differential and its permanent effects on pin-to-hole tolerance must be implemented into design solutions.

A design goal of the filament-wound case program is that all segments be capable of reuse for four flights. This requires recycling through all the environments of refurbishment, hydroproofing, liner vulcanization, flight, water splash, and soak. How the laminate elastic properties, joint tolerances, and local strains [2] degrade and affect the axial and bending stiffness of the solid rocket motor case through recycling could only be assessed by an extensive test program.

The nature of joint axial elongation due to pin-to-hole tolerances and high local strains may be envisioned as a short weak spring in series with the membrane stiffness. Uncertainties in joint behavior or any relaxation in manufacturing or refurbishment control on tolerance must be compensated by increasing the laminate membrane axial stiffness at the expense of payload performance; provided the ramp excitation does not degenerate into a step function.

Recognizing the diversity of elastic properties obtainable from filament-wound shells through the control of numerous parameters evolving from the manufacturing process, it was considered essential to determine the more significant parameters affecting the membrane axial growth and assess their growth dispersions based on the experienced variation of these parameters. A sensitivity analysis was performed on the optimized laminate design that went beyond equation (2), into the micromechanics model, to identify the independent variables. It was discovered that the helical fiber modulus accounted for over 50 percent of the bending stiffness and 80 percent of the axial growth and that the winding angle was the only other important variable. A coefficient of variation of only 2 to 3 percent in these two variables resulted in a 15 percent variation on the axial growth. These results provided a basis for developing fiber acceptance criteria and winding angle inspection standards for this unique laminate requirement. The sensitivity analysis results were then used as input to the dispersion analysis to predict 2-sigma deviations required by the system's loads.

Over 30 bottles of the selected filament-wound case system were fabricated early in the test program to verify the analytically predicted nominal axial growth and dispersions during the design phase. Later axial growth of all deliverable motor case segments are required to be verified by test including joint effects. Refurbished segments must be tested during hydroproof for compliance with axial-growth specified allowables. A sonic velocity method is planned for verifying the axial and hoop moduli of all deliverable filament-wound segments. However, this method is not applicable for verifying those moduli on the smaller laminate bottle test specimen. Therefore, a nondestructive test analysis technique was conceived to obtain the constitutive relations and dispersions of a specially orthotropic laminate from pressurized cylindrical bottle specimen. This technique should prove useful for recording changes in elastic properties during pressure cycling. It should also be applicable as a backup or second source to the sonic method planned for deliverable laminate segments and be especially useful to back out the Poissons' ratio which the sonic method cannot achieve.

6

EXTENSIONAL PROPERTIES VERIFICATION METHOD

The optimized membrane of each filament-wound case segment consists of numerous hoop layers of graphite fibers interspersed with balanced helical layers that are symmetrically wound with the middle surface and with the cylinder axis. This represents a "specially orthotropic laminate" for which the in-plane extensional properties are simplified. During the design phase of the filament-wound case, the axial, hoop, and shear moduli and the Poisson's ratio were predicted by the classical thin laminate theory. But before committing the fabrication of full-scale segments, small cylindrical pressure vessels are usually constructed of the same laminate system and with the same processing controls to verify that indeed these extensional properties and dispersions are as predicted.

Clearly, the objective of the pressure vessel test is to translate the vessel geometry, the recorded hydropressure, P, and corresponding surface displacements into extensional properties. At a distance away from the end closure discontinuities, no shearing stresses act on the cylindrical membrane due to symmetry of the laminate, the vessel geometry and the pressure loading. Therefore, the only stresses experienced by the laminate are biaxial in proportion to

$$\sigma_1 = \frac{\sigma_2}{2} = \frac{PD}{4t} \tag{3}$$

where subscripts 1 and 2 refer to axial and hoop directions, respectively. The mean diameter, mean thickness, and tolerances are attainable from the specimen drawings.

Surface displacements of small specimen are most efficiently measured with electrical strain gauges. Notwithstanding, the nature of filament-wound surfaces compels the use of large gauge extensometers as the primary test data source. Axial and girth orientation of the planned extensometers conform to the following constitutive relationship.

$$\begin{Bmatrix} \epsilon_1 \\ \epsilon_2 \\ \gamma_{12} \end{Bmatrix} = \begin{bmatrix} S_{11} & S_{12} & 0 \\ S_{12} & S_{22} & 0 \\ 0 & 0 & S_{66} \end{bmatrix} \begin{Bmatrix} \sigma_1 \\ \sigma_2 \\ \tau_{12} \end{Bmatrix}$$

Substituting the specimen specific conditions discussed, the constitutive relationship provides two constraint equations with three unknown parameters expressed by

$$C_1 = S_{11} + 2 S_{12} \tag{4a}$$

$$C_2 = S_{12} + 2 S_{22} \tag{4b}$$

The three unknown parameters are the engineering constants

$$S_{11} = \frac{1}{E_{11}} \quad ; \quad S_{22} = \frac{1}{E_{22}} \quad ; \quad S_{12} = -\frac{\nu_{12}}{E_{11}} \quad , \tag{5}$$

that include the desired extensional properties to be determined from the test and then to be compared with the predicted design properties. The constants

$$C_1 = \frac{\epsilon_1}{\sigma_1} = \frac{4t}{D} \frac{\epsilon_1}{P} \quad , \tag{6a}$$

$$C_2 = \frac{\epsilon_2}{\sigma_1} = \frac{4t}{D} \frac{\epsilon_2}{P} \quad , \tag{6b}$$

are determined from test data of axial and hoop strains, ϵ_1 and ϵ_2, respectively, corresponding to the hydrostatic pressure. Accuracy of test results is subject to an error analysis based on the precision of the test instrumentation.

A third equation may be formulated from the principle of least squares [3]. Accordingly, the most probable values of the observed engineering constants, S_{ij}, are those for which the sum of the squares of the differences between the observed and the predicted engineering constants A_{ij} results is the smallest possible. This principle may be expressed in functional form by

$$f(S_{ij}) = (A_{11} - S_{11})^2 + (A_{22} - S_{22})^2 + (A_{12} - S_{12})^2 = min. \quad , \tag{7}$$

where A_{ij} are the design predicted engineering constants defined similarly to those observed by equation (5).

It is known from differential calculus that a constant (λ) exists called the Lagrange Multiplier [4] that will minimize the functional equation and satisfy the constraint (g) equations such that

$$\frac{\partial f}{\partial S_{ij}} = \frac{\partial}{\partial S_{ij}} [f(S_{ij}) + \sum \lambda_n g_n] = 0 \quad .$$

Substituting equations (7), (4a), and (4b) gives

$$\frac{\partial}{\partial S_{ij}} [(A_{11} - S_{11})^2 + (A_{22} - S_{22})^2 + (A_{12} - S_{12})^2 + \lambda_1 (S_{11} + 2 S_{12} - C_1)$$

$$+ \lambda_2 (S_{12} + 2 S_{22} - C_2)] = 0 \quad .$$

Making it stationary with respect to the constrained engineering constants, S_{ij}, gives

$$\frac{\partial f}{\partial S_{11}} = - 2 (A_{11} - S_{11}) + \lambda_1 = 0 \qquad\qquad (9a)$$

$$\frac{\partial f}{\partial S_{22}} = - 2 (A_{22} - S_{22}) + 2 \lambda_2 = 0 \quad , \qquad\qquad (9b)$$

$$\frac{\partial f}{\partial S_{12}} = - 2 (A_{12} - S_{12}) + 2 \lambda_1 + \lambda_2 = 0 \quad . \qquad\qquad (9c)$$

Equations (4) and (9) constitute five linear homogeneous equations in as many unknowns. Solving simultaneously yields the hoop engineering constant,

$$S_{22} = \frac{2}{21} (5 C_2 - 2 C_1) + \frac{1}{21} (4 A_{11} + A_{22} - 2 A_{12}) \quad , \qquad\qquad (10)$$

which is substituted into

$$S_{11} = 4 S_{22} - 2 C_2 + C_1 \quad . \qquad\qquad (11)$$

and

$$S_{12} = C_2 - 2 S_{22} \quad , \qquad\qquad (12)$$

to complete the solution of three observed engineering constants.

It was noted that the shear modulus (S66) was not verifiable from this test configuration though its effects are intrinsic to the verifiable moduli. However, its observed value is necessary for modal modeling of the solid rocket structure and a more appropriate shear modulus test should be performed on a subscale model which includes joints such as the quarter-scale dynamic test segments provided in the program.

9

It was also noted that the strains discussed were oriented in hoop and axial directions only. Should the strains be measured at some arbitrary angles, then the constitutive relationship must be transformed to the arbitrary set of axes and the matrix components would contain shear modulus properties of the helical laminae. Verification of properties by the above method is applicable but would become laborous and less accurate.

FILAMENT-WOUND CASE DYNAMICS

Shuttle system interface loads are dominated by liftoff dynamics of which the rocket motor case axial and flexural stiffnesses are two interacting properties that were altered by the laminate substitution. Therefore, the modified case stiffness was assessed with the totally integrated structural system. A preliminary structural dynamics analyses of the modified case stiffness had no major influence on the Shuttle elements and interface loads.

The laminate motor case bending modulus was reduced to 66 percent of the existing steel case and the natural lower bending frequencies decreased only 16 percent. All lower modes were bending and axial. The first torsional mode was associated with a local shell mode at the external tank aft attachment. This shell mode occurred primarily in the steel segment and should transmit only minor effects to adjacent laminate segments. Therefore, retention of the steel segment interface was particularly prudent since it minimized the laminate stiffness effect on the local shell mode, with potential flexure discrepancies noted [5,6] between calculated and observed frequencies, that is coupled with the nonlinear differential stiffness [7] related to the internal pressures.

Two quarter-scale replica of the filament-wound motor case are provided in the dynamics test program. One test article will be used to simulate burn-out case dynamics while the second will be loaded with inert propellant to simulate liftoff dynamics. These tests will be used to verify structural dynamic math modeling predictions of the filament-wound case as was earlier done with the quarter-scale steel motor case. The data base and experience developed during prior steel case dynamics test may help to readily account for composite dynamic effects.

CONCLUSION

The high specific strength and modulus of graphite-epoxy laminate made it an expedient material substitute for the Shuttle solid rocket motor steel case. Its implementation substantially increased the payload performance with no changes in physical interfaces between elements and major existing components. Because of the wide range and variety of elastic properties obtainable through simple changes in wind angles, mixes, and layer arrangements, the Shuttle system's interface loads were not exceeded.

However, the laminate system design was subjugated to the unique axial elongation constraint from the beginning. The increased complexity of joints between segments and domes, the increased need for pins and associated tolerances, and the increased hole elongation aggravated the axial growth of the laminate motor case. It was resolved by increasing the Poisson's ratio with a notable weight increase over that required to only satisfy the case integrity.

This filament-wound case program demonstrated the sometimes commandeering role of structural dynamics on laminate system design which is more often optimized by the stress domain. It also demonstrated a need for establishing test methods to verify or determine elastic properties for laminated, pressurized vessels.

REFERENCES

1. Ryan, R. S., et al.: System Analysis Approach to Deriving Design Criteria for Space Shuttle and its Payloads. NASA Technical Paper No. 1949, December 1981.

2. Pyner, G. R. and Matthews, F. L.: Comparison of Single and Multi-Hole Bolted Joints in Glass Fiber Reenforced Plastic. Composite Materials, July 1979.

3. Sokolnikoff, I. S. and Redheffer, R. M.: Mathematics of Physics and Modern Engineering. McGraw-Hill, 1966.

4. W. Flugge: Handbook of Engineering Mechanics. McGraw-Hill, 1962.

5. Crawley, E. F.: The Natural Mode of Graphite/Epoxy Cantilever Plates and Shells. Composite Material, July 1979.

6. Ashton, J. E. and Waddoups, M. E.: Analysis of Anistrope Plates. Composite Materials, January 1969.

7. Przemienieck, J. S.: Theory of Matrix Structural Analysis. McGraw-Hill, 1968.

1. REPORT NO. NASA TP-2117	2. GOVERNMENT ACCESSION NO.	3. RECIPIENT'S CATALOG NO.
4. TITLE AND SUBTITLE Identification and Management of Filament-Wound Case Stiffness Parameters		5. REPORT DATE January 1983
		6. PERFORMING ORGANIZATION CODE
7. AUTHOR(S) V. Verderaime and M. Rheinfurth		8. PERFORMING ORGANIZATION REPORT #
9. PERFORMING ORGANIZATION NAME AND ADDRESS George C. Marshall Space Flight Center Marshall Space Flight Center, Alabama 35812		10. WORK UNIT NO. M-403
		11. CONTRACT OR GRANT NO.
		13. TYPE OF REPORT & PERIOD COVERED
12. SPONSORING AGENCY NAME AND ADDRESS National Aeronautics and Space Administration Washington, D.C. 20546		Technical Paper
		14. SPONSORING AGENCY CODE

15. SUPPLEMENTARY NOTES

Prepared by Systems Dynamics Laboratory, Science and Engineering Directorate.

16. ABSTRACT

   The high specific strength and the high specific modules made graphite-epoxy laminate an expedient material substitute for the Shuttle Solid Rocket Motor steel case to substantially increase the payload performance without increasing the composite case axial growth during thrust build-up which was constrained to minimize liftoff excitation effects on existing structural elements and interfaces. Parameters associated with axial growth were identified for quality and manufacturing controls. Included is an innovative method for experimentally verifying extensional elastic properties on a laminate pressurized test bottle.

17. KEY WORDS Graphite filament pressure vessel Composite constitutive verification Composite axial growth parameters Composite solid rocket motor case	18. DISTRIBUTION STATEMENT Unclassified – Unlimited Subject Category 24		
19. SECURITY CLASSIF. (of this report) Unclassified	20. SECURITY CLASSIF. (of this page) Unclassified	21. NO. OF PAGES 17	22. PRICE A02

National Aeronautics and
Space Administration

Washington, D.C.
20546

Official Business
Penalty for Private Use, $300

THIRD-CLASS BULK RATE

U.S.MAIL

NASA